Article

Functionalizing Surfaces by Physical Vapor Deposition To Measure the Degree of Nanoscale Contact Using FRET

Mónica Gaspar Simões,* Katrin Unger, Caterina Czibula, Anna Maria Coclite, Robert Schennach, and Ulrich Hirn

Read Online

ACCESS | Metrics & More | Article Recommendations | SI Supporting Information

ABSTRACT: Adhesion between solid materials is caused by intermolecular forces that only take place if the adhering surfaces are at nanoscale contact (NSC) (i.e., 0.1−0.4 nm. To study adhesion, NSC can be evaluated with Förster Resonance Energy Transfer (FRET). FRET uses the interaction of compatible fluorescence molecules to measure the nanometer distance between bonded surfaces. For this, each surface is labeled with one fluorescence dye, named the Donor or Acceptor. If these molecules are in NSC, a nonradiative Donor−Acceptor energy transfer will occur and can be detected using FRET spectroscopy.

Here, for the first time, we introduce an innovative concept of a FRET-based NSC measurement employing dye-nanolayer films prepared by a physical vapor deposition (PVD). The dye nanolayers were prepared by PVD from the vaporization of the Donor and Acceptor molecules separately. The selected molecules, 7-Amino-4-methyl-cumarin (C120) and 5(6)-Carboxy-2′,7′-dichlor-fluorescein (CDCF), present high quantum yields (QY, $QY_D = 0.91$ and $QY_A = 0.64$) and a low FRET distance range of 0.6−2.2 nm, adequate for the study of NSC. The produced dye-nanolayer films exhibit a uniform dye distribution (verified by atomic force microscopy) and suitable fluorescence intensities. To validate the NSC measurements, FRET spectroscopy experiments were performed with bonded dye-nanolayer films prepared under different loads (from 1.5 to 140 bar), thus creating different degrees of NSC. The results show an increase in FRET intensity ($R^2 = 0.95$) with the respective adhesion energy between the films, which is directly related to the degree of NSC. Hence, this work establishes FRET as an experimental technique for the measurement of NSC, and its relation to surface adhesion. Additionally, thanks to the FRET dye-nanolayer approach, the method can be employed on arbitrary surfaces. Essentially, any sufficiently transparent substrate can be functionalized with FRET compatible dyes to evaluate NSC, which represents a breakthrough in contact mechanics investigations of soft and hard solid materials.

KEYWORDS: adhesion, nanoscale contact, FRET spectroscopy, physical vapor deposition, dye-nanolayer, fluorescence
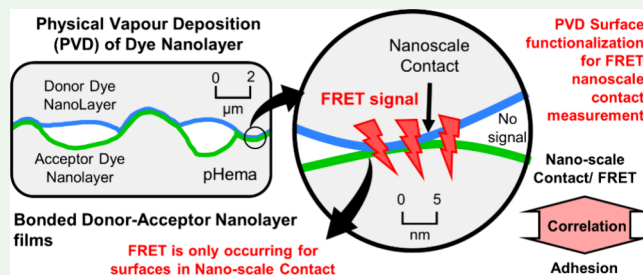
INTRODUCTION

Measurement of NSC between Surfaces Using FRET. Surface adhesion is essential in several engineering applications, contact mechanics, and biological systems.[1−3] Some basic examples where adhesion plays a role are car tires sticking to the road and geckos walking on the wall. This phenomenon is caused by intermolecular forces, like hydrogen bonds and van der Waals interactions, that only take place if the adhering surfaces are in nanoscale contact (NSC), i.e. 0.1−0.4 nm.[4−8] Therefore, the adhesion between two surfaces is proportional to its NSC area, and can only be properly investigated if the associated degree of NSC is correctly evaluated.[9] However, we still cannot gain insight into it due to the physical difficulties of looking directly at the NSC. Here, we tailored a FRET-based experimental technique to enable access to NSC and provide a quantification approach.

FRET (Förster Resonance Energy Transfer) has recently been introduced as an experimental technique for the measurement of NSC between soft surfaces.[10−12] FRET takes advantage of the fluorescence properties of specific compatible molecules to determine their exact nanometric distance (0−20 nm).[13] Thus, if these molecules, named Donor and Acceptor, are in NSC, a nonradiative Donor → Acceptor energy transfer will occur and a FRET signal can be detected.[14,15] The FRET distance range depends on the Förster Radius (R_0) of the FRET dyes utilized and can only be properly sensed between $0.5R_0$ and $2R_0$.[14] Above $2R_0$, the Donor and Acceptor molecules are simply too distant for a FRET interaction. And below $0.5R_0$ the dyes are too close to each other, which can lead to orbital overlapping and electron exchange (so-called Dexter transfer)[16] resulting in an energy
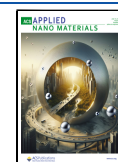
transfer in both directions: Donor ↔ Acceptor, which invalidates any FRET measurement.[15,16]

To employ this technique for NSC between surfaces, each interface needs to be labeled with the Donor or Acceptor dye (Figures 1 and S1).[10] Due to the natural roughness of any
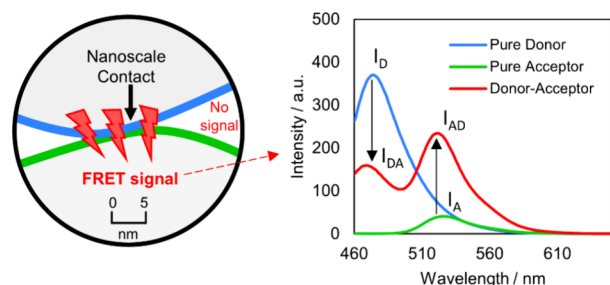

Figure 1. Two surfaces are in close contact with areas in NSC. FRET signal with the pure Donor (I_D) and Acceptor (I_A) without NSC between the dye. In the case of NSC, Donor intensity drops (from I_D to I_{DA}) and Acceptor intensity rises (from I_A to I_{AD}) due to the Donor−Acceptor energy transfer (see arrows). Adapted from ref 10. Copyright 2021 American Chemical Society.

surface, the NSC is not complete.[17] Instead, areas that look to be in full contact at the microscale end up revealing opens gaps at the nanometric scale.[18] Thus, the areas in the NSC are regularly overestimated when contact is evaluated at lower magnifications. However, a FRET signal only occurs within areas in NSC ($0.5R_0−2R_0$), for the open gaps above $2R_0$ no FRET can be found (Figures 1 and S1). Hence, FRET is a suitable technique to directly evaluate the degree of NSC between surfaces.[15] In practice, the surfaces in NSC can be analyzed by FRET spectroscopy to follow the spectral effect of FRET on the Donor and Acceptor molecules. A FRET signal (Figure 1) can be identified by a change in the fluorescence signal of the two dyes. Comparing the spectra of the individual dye surfaces (blue and green lines) to the spectrum of the surfaces in contact (red line), the Donor intensity decreases (from I_D to I_{DA}), and Acceptor intensity increases (from I_A to I_{AD}) due to the Donor → Acceptor energy transfer (FRET). Through the FRET signal, i.e. the Acceptor intensity increase from I_A to I_{AD} (Figure 1), it is possible to calculate the FRET efficiency (FRETeff),[14,15] which indicates the degree of NSC.

Recently it has been demonstrated that the NSC measured with FRET correlates to the adhesion between soft materials.[10−12] These studies showed that for bonded thin films pressed under different loads, the FRETeff and adhesion increase with the applied pressure, caused by the correspondent increase of the degree of NSC.[10] Thus, FRET has been introduced as a proper technique to quantify the degree of NSC and establish a relation between FRETeff and adhesion in bonded films.

PVD of FRET-Dye Nanolayers to measure NSC between Arbitrary Surfaces. In the original proof-of-concept studies, the fluorescent dyes were mixed in soft, thin films, which allow us to produce uniform and well distributed dye films, use exact dye concentrations, and study/develop different FRET systems for the measurement of NSC. This, however, is strongly limiting the applicability of the method to polymer surfaces where the fluorescence molecules must be solubilized in the polymer solution.[10−12] Moreover, utilizing these films, the dye molecules were present not only in the interface between the thin films, where FRET can occur within

$0.5R_0−2R_0$, but also through the entire polymeric matrix of the thin films (Figure 2A). This leads to a strong increase of the
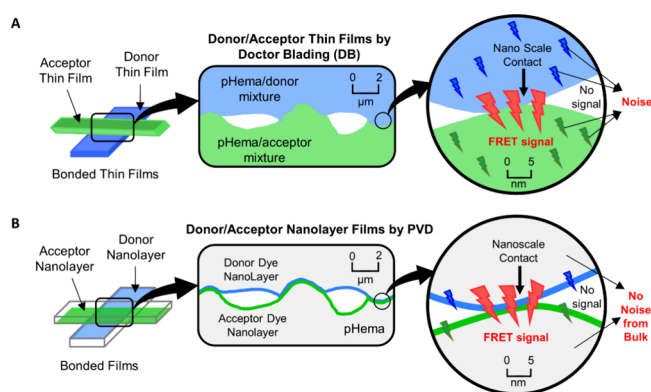
Figure 2. Bonded films in close contact observed at the micrometer and nanometer scale. Contact area decreases with increasing magnification. For areas in NSC, a FRET signal can be detected. Above the FRET distance range of the system, the transfer of energy does not occur. There is no FRET signal. (A) Donor and Acceptor bonded thin films prepared by DB, where the dyes were previously dissolved in the films.[10−12] Donor and Acceptor molecules can be found through the entire bulk of the film (1.5 μm thickness), and excess fluorescence intensity (not FRET related noise) is detected during the FRET measurements; (B) Donor- and Acceptor nanolayer bonded films prepared by PVD. The dyes can only be found on the material surface, where the NSC and FRET occur. No fluorescence noise from the bulk is detected. Adapted from ref 10. Copyright 2021 American Chemical Society.

pure dyes' spectral signal which makes it harder to detect the FRET signal, which is the Acceptor intensity _increase_ from I_A to I_{AD} (see Figure 1), creating a low signal-to-noise ratio[19] in the system.

Therefore, the most suitable system should only have Donor and Acceptor molecules on the interface of the films (Figure 2B), to reduce the noise from the matrix below the surfaces, thus enhancing the sensitivity of the method[20] for the measurement of NSC and associated adhesion.

In this work, we develop an innovative FRET system with dye-nanolayer films, prepared by physical vapor deposition (PVD). PVD is a coating technique mostly utilized in nanoscience for the fabrication of functional nanolayers, where the molecules are vaporized and condensate over a substrate at the atomic level employing a combination of high vacuum and temperatures.[21−23] It can be used to form single-crystalline Si layers on glass substrates,[24] metal monolayers for semiconductors[25] or biosensors, and surface modifications.[26]

For this research, the Donor and Acceptor molecules are separately vaporized and deposited over clean polymeric thin films. By functionalizing the films with this approach, all dye molecules are concentrated at the surface and noise from the bulk will not occur (Figure 2B). Moreover, any Donor and Acceptor molecules with low saturation pressure can be deposited over other types of transparent substrates, enhancing the applicability of the method.

For the experiments we used a FRET pair, specially designed by us for the measurement of NSC.[11,12] The FRET pair is composed of 7-Amino-4-methyl-cumarin (C120, Figure 3A) as the Donor dye and 5(6)-Carboxy-2′,7′-dichlor-fluorescein (CDCF, Figure 3B) as the Acceptor dye. Both molecules present high quantum yields (QY, $QY_D = 0.91$ and $QY_A = $
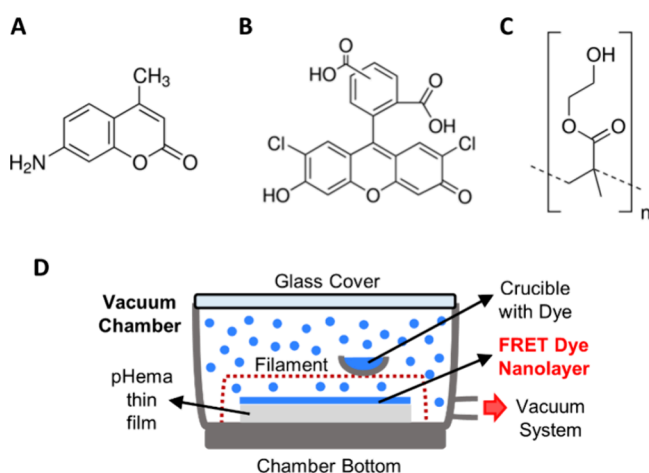
Figure 3. (A) Donor, C120; (B) Acceptor, CDCF; (C) pHema (thin films material) chemical structures; and (D) schematic representation of the PVD chamber used for the preparation of the dye-nanolayers.

0.64) and a FRET distance range from 0.6 to 2.2 nm (at 0.1 mM), suitable for the study of NSC and adhesion caused by intermolecular forces that only occur at low nanometric distances (below 1 nm). The C120 and CDCF nanolayers are deposited over poly(2-hydroxyethyl methacrylate) (pHema, Figure 3C) thin films by PVD (Figure 3D).

To validate our PVD-based approach, we are bonding the films carrying the donor- and acceptor-nanolayer with increasing pressure, creating increasing degrees of NSC, and subsequently increasing adhesion. Therefore, the degree of NSC is the only driving force for the change in adhesion. Linking the NSC measured with FRET to the adhesion between the dye-nanolayer films (by evaluating the separation energy in tensile testing), we are proving the expected relation between FRET and adhesion, employing an original FRET system specially developed to evaluate surface interactions at short nanometric distances with high precision.

■ RESULTS AND DISCUSSION

To apply our FRET method on arbitrary surfaces, we developed an innovative FRET system based on dye-nanolayer films was developed. The dye nanolayers were prepared by PVD from the vaporization of the Donor and Acceptor molecules[22] and applied to pHEMA thin film surfaces (considering that any sufficiently transparent substrates can be functionalized with a dye-nanolayer of FRET dyes to evaluate NSC and surface adhesion).

The FRET dyes employed in this work, C120 and CDCF as FRET dyes, with a high quantum yield and small spectral overlap, which results in a low Förster Radius (2.2 nm at 0.1

mM) and FRET distance range (0.6−2.2 nm),[11,12] also present a low vapor pressure of the molecules that they could be vaporized in the PVD. This pair of FRET dyes was specifically designed to study interactions that occur at short nanometric distances, as is the case for the intermolecular forces responsible for adhesion.

Here, bonded donor−acceptor nanolayer films were prepared under a series of different loads to measure FRET. With this, the main objective was to create different degrees of NSC and adhesion, since the nanometric distance between the soft/pressure-sensitive films is decreasing in the function of the applied load.

Later, the resulting FRET signals were compared to the energy necessary to separate the bonded dye-nanolayer films in Z-direction tensile tests, therefore, validating the designed system as an appropriate FRET method for the measurement of NSC.
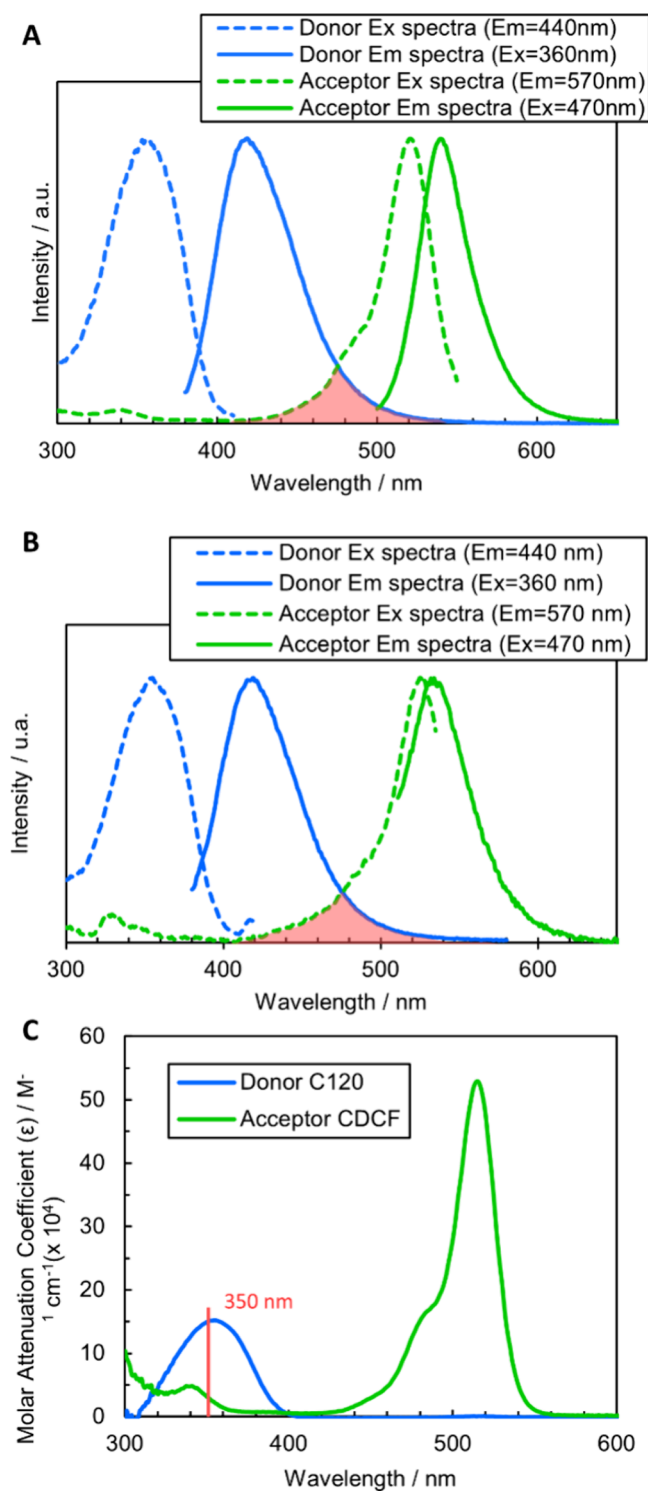
Dye Nanolayer Films. The dye-nanolayer films used in the FRET experiments consisted of a substrate (pHema thin film) and a dye (donor or Acceptor) nanolayer. Accordingly, the films were prepared in two steps: (1) 1.5 μM pHema thin films were formed by doctor blading, and (2) the dye-nanolayers were deposited over the pHema thin films by PVD. For the deposition, the Donor and Acceptor molecules were vaporized using a combination of high temperatures (substrate at 60 °C and filament at 100/120 °C) and low pressure (100 mTorr) in a custom-built PVD chamber, as demonstrated in Figure 3D (all details in the Materials and Methods PVD section), without compromising the pHema thin films integrity (transition temperature above 80 °C).

After the procedures, the surface of the untreated and treated films was analyzed by atomic force microscopy (AFM). Figure 4 shows the topography of the original pHema thin film (A) and the donor-nanolayer (B) and acceptor-nanolayer (C) films. The topography looks similar (Figure 4A-C), and their correspondent root-mean-square (RMS) roughness (A: 0.30 ± 0.15 nm; B: 0.30 ± 0.05 nm and C: 0.25 ± 0.05 nm, values are average in the ±95% confidence interval, n = 3) are equivalent, showing that the PVD procedure did not alter the surface morphology of the films, which indicates that the deposited dye-nanolayers are uniform and well distributed and no significant surface artifacts like, for example, dye aggregates had been formed by the PVD application.

When the spectra of C120 and CDCF dissolved in pHema (Figure 5A) are compared with the PVD nanolayer films spectra (Figure 5B), both present similar excitation and emission intensity peaks. The Donor fluorescence spectra are virtually the same, and only the Acceptor spectra show an ~10 nm wavelength shift to the left (Figure 5A and 5B). In the Acceptor-nanolayer film, the excitation and emission spectra are closer to each other. Fluorescent wavelength shifts of the
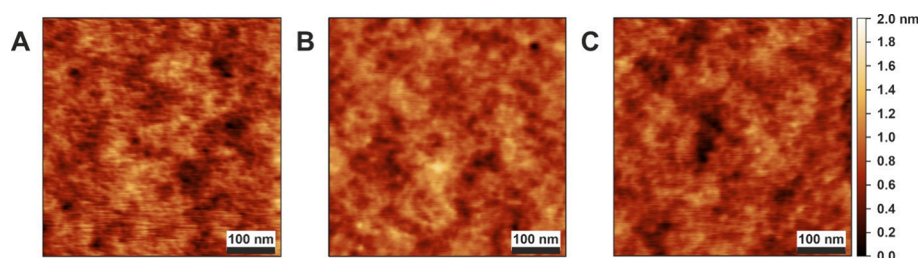
Figure 4. 500 × 500 nm² AFM topography images of the (A) pHema, (B) donor-nanolayer, and (C) Acceptor-nanolayer films.

Figure 5. Excitation and emission fluorescence spectra of the (A) Donor- and Acceptor-dissolved pHema thin films and (B) Donor- and Acceptor-nanolayer films. The spectral overlap between Donor emission and Acceptor excitation is marked in orange. (C) Molar attenuation coefficient (ε) spectra of the Donor- and Acceptor-dissolved pHema thin films. For FRET measurements, the samples were excited at 350 nm ($\varepsilon_A/\varepsilon_D = 0.21$).

same molecules in different surrounding media, concentration, and thickness (light path) are expected.[27]

This may have been caused by the long exposure to high temperatures and low vacuum pressure during PVD, which can

interfere with the substrate transparency and fluorescence spectra precision. Another possible explanation is the large size of the Acceptor molecules (see Figure 3B), making them harder to vaporize and distribute than the Donor, complicating the formation of a smooth dye-nanolayer. However, the AFM images demonstrate a low and similar roughness for all films.

Eventually, there is the possibility of some chemical interaction between the dyes and pHema, and its effects on the fluorescence spectra should not be discarded. During PVD no initiator or catalyzer was used to enhance the reactivity of the molecules. However, the C120 and CDCF molecules (Figure 3A−C) present several reactive groups (C120: −CH$_3$ and −NH$_2$; and CDCF: −Cl, −OH, and −COOH) available to react with the pHema (containing −OH and −COOH reactive groups). In particular, the −NH$_2$ and −Cl in C120 and CDCF, respectively, are placed in the extremities of the molecules and are less stable/more reactive at higher temperatures and low pressure, as in the PVD procedure applied in this study. Therefore, we cannot confirm or deny any chemical bonding between the deposited nanolayer of dye molecules and the pHema surface, particularly the Acceptor one. Nevertheless, the dye-nanolayer films present a spectral overlap between the Donor emission and Acceptor excitation spectra (Figure 5B, marked in orange), on which FRET depends. That is identical to the one observed in the dye-dissolved pHema films (Figure 5A, marked in orange), demonstrating their equal capacities for FRET.

In summary, we have demonstrated that PVD is working for the functionalization of substrate surfaces with extremely thin layers (thickness was not possible to measure with profilometry) of FRET dyes. Yet, spectroscopic character-ization revealed that the Donor and acceptor nanolayers fulfill the requirements to produce a FRET signal when being brought to a close distance around the estimated Förster Radius of 1 nm.

FRET Measurements. The FRET nanolayer system was analyzed by FRET spectroscopy. For this, the Donor and acceptor nanolayer films were bonded together with several ascending loads, from 1.5 to 140 bar. Increasing the pressure leads to an increase in the degree of NSC and a subsequent increase in adhesion. The samples were produced by bonding pure Donor-nanolayer (D), pure Acceptor-nanolayer (A), and no dye/clean pHema (H) films, as demonstrated in Figure 6A-C. D/H, H/A, and D/A are the Donor−pHema, Acceptor−pHema, and Donor−Acceptor thin film combinations, respectively (Figure 6A−C). In the fluorescence spectrometer, all experiments were carried out keeping a consistent arrangement of the films, with Acceptor in the front and Donor in the back position in relation to the light source, which was in a 45°/45° configuration (Figure 6C).

As the molar concentration of the dyes in the nanolayer films is unknown, for these FRET experiments we used the molar attenuation coefficient spectra (ε) of the Donor and Acceptor thin films with dyes dissolved in pH 0.1 mM (Figure 5C). The ε spectra are necessary to identify the wavelength intervals where both dye molecules can be excited using the same excitation wavelength, which is a FRET requirement.[14,15] Moreover, the ratio $\varepsilon_A/\varepsilon_D$ is later used to determine the FRETeff (eq 3), which is the measure for the detected FRET signal and, hence, the degree of NSC.[14,15] The FRET excitation wavelength must be selected to have a high ε_D because the Donor molecules need enough light to be excited and transfer energy to the Acceptor. On the contrary, ε_A must
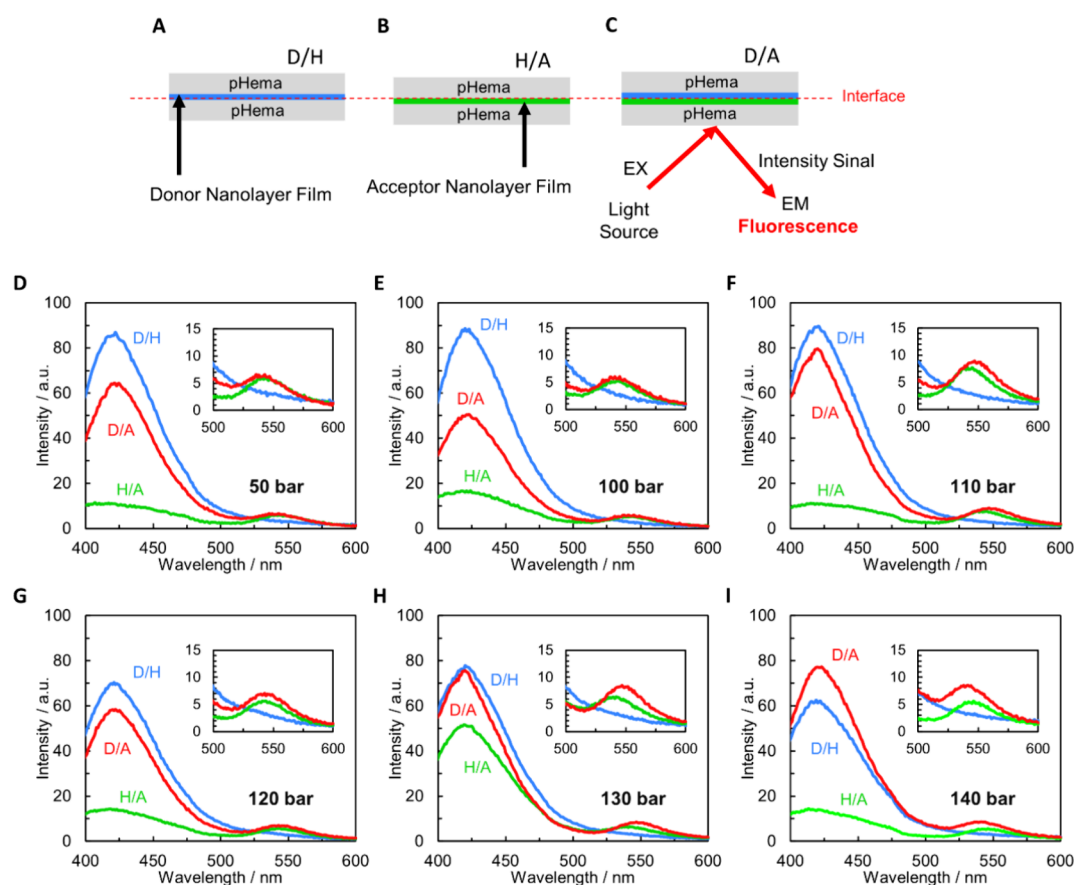
Figure 6. Bonded dye-nanolayer films: (A) Donor/pHema (D/H), (B) pHema/Acceptor (H/A), and (C) Donor/Acceptor (D/A). And emission fluorescence spectra of the Donor- and Acceptor-nanolayer bonded thin films with increasing bonding pressure of (D) 50 bar, (E) 100 bar, (F) 110 bar, (G) 120 bar, (H) 130 bar, and (I) 140 bar (excited at 350 nm, $\varepsilon_A/\varepsilon_B = 0.21$).

be lower since the Acceptor will receive extra energy from the Donor. Still, ε_A cannot be too low since it also needs to be excited for the FRET. Accordingly, the fluorescence spectra for the dye-nanolayer films were collected at 350 nm excitation, where the ratio $\varepsilon_A/\varepsilon_D = 0.21$ (see Figure 5C).

Figure 6D-I depicts the bonded donor/acceptor nanolayer film emission spectra bonded together with pressures from 50 to 140 bar. From 50 to 130 bar (Figure 6D-H) a standard FRET performance, with Donor Quenching (from I_D to I_{DA}, Figure 1) and Acceptor Sensitization (from I_A to I_{AD}, Figure 1), can be observed. However, a shift from the normal Donor-FRET behavior can be noticed at a bonding pressure of 140 bar (Figure 6I). Here, the Donor intensity increases when in the presence of the Acceptor (D/A spectra in relation to D/H spectra in Figure 6I), against what is expected during FRET due to the Donor → Acceptor energy transfer (Figure 1). This phenomenon can occur when the Donor and Acceptor molecules are too close to each other, below $0.5R_0$; it is called Dexter Transfer.[28,29] Being so close, there is a high chance of orbital overlapping, which can result in electron exchange between the Donor and Acceptor molecules, and energy transfer in both directions occurs: Donor ↔ Acceptor. Thus, instead of a traditional FRET Donor intensity decrease, caused by Donor quenching (Figure 6D-H) we have the Donor intensity rise as can be observed in Figure 6I.

The fact that we can observe Dexter transfer with this FRET system may be related to the dye-nanolayer films. Because in this further approach, the Donor and Acceptor molecules are no longer distributed through the entire polymeric matrix of

the thin films (Figure 2A), but only on the pHema surface (Figure 2B). Thus, all the dye-nanolayer molecules are concentrated in the interface between the bonded films, accessible for FRET and physically closer, which can explain the presence of Dexter transfer (contact below $0.5R_0 = 0.6$ nm) within films bonded under 140 bar (Figure 6I). This result confirms the sensitivity of the method due to the development of a FRET pair/system specially designed and optimized for the measurement of NSC. Considering that no dye migration or interdiffusion at these pressure conditions (room temperature) is observed, the transfer of energy occurs only on the interface between the dye-nanolayer films, and the FRET signals derive exclusively from their proximity, i.e., NSC.

Nevertheless, from 1.5 to 130 bar a standard FRET performance, with Donor Quenching and Acceptor Sensitization, can be observed (Figure 6D-I and Table 1). The FRETeffs from 1.5 to 140 bar (Table 1) were calculated with the Acceptor sensitization method (eq 4), which only relies on the Acceptor molecule's response to the nanometric presence and proximity of the Donor dye.[10,30,31] For 1.5 bar, the measured FRETeff was 0%, indicating no NSC within $0.5R_0$–$2R_0$. On the other hand, for 130 bar the FRETeff was ~6% (Table 1), a high FRET signal intensity, especially considering that the molar concentration of the dyes is low (below 0.1 mM) and nonequal.

Analyzing the fluorescence spectra, FRET signals, and FRETeffs altogether (Figure 6D-I and Table 1), our experiments reveal that when the pressure to bond the Donor/

Table 1. FRET Signal Intensity (FRETeff), Maximum Tensile Force, and Separation Energy Per Unit Area of the Bonded Nanolayer Films under Different Loads[a]

D/A Bonding Pressure (bar)	FRETeff (%)	Maximum Tensile Force (N)	Separation Energy per Unit Area (mJ/cm²)
1.5	0	10.3 ± 0.5	0.05 ± 0.00
50	2.5 ± 0.6	20.2 ± 2.8	0.13 ± 0.02
100	3.1 ± 0.8	30.0 ± 3.0	0.24 ± 0.03
110	3.3 ± 0.9	39.8 ± 3.6	0.35 ± 0.04
120	4.9 ± 0.7	47.8 ± 5.5	0.45 ± 0.07
130	5.9 ± 0.9	52.2 ± 0.7	0.51 ± 0.01
140	10.2 ± 1.2	76.3 ± 3.8	0.84 ± 0.05

[a]Values are averages ±95% confidence interval ($n = 3$ for FRET efficiency, and $n = 4$ for tensile force and separation energy).

Acceptor-nanolayer films increases, the FRET signals and their relative FRETeffs also increase accordingly.

Correlation between NSC and Adhesion. To validate the measurement of NSC using FRET, we measured the adhesion between the nanolayer films, which was created by the NSC between the surfaces, and correlated it to the measured FRET signals. Thus, the bonded films were separated by *z*-directional tensile testing to determine the separation energy and maximum adhesion force. The results showed that both parameters increase, with the increasing pressure applied to bonded dye-nanolayer films (Table 1), due to a higher degree of NSC and adhesion force. The separation energy per unit area was calculated by the integral of the tensile test force−displacement curves (Figure S2). The bonded surface FRETeffs and corresponding adhesion (separation energy per unit area) were plotted together in Figure 7.
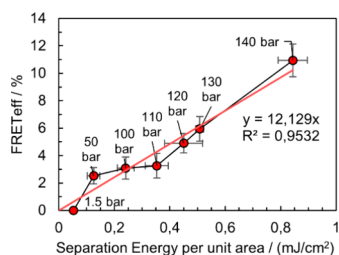
Figure 7. FRETeff as a function of the adhesion (separation energy per unit area) between the Donor/Acceptor bonded nanolayer films pressed with 1.5 to 140 bar. Values are average ±95% confidence interval ($n = 3$ for FRET efficiency and $n = 4$ for tensile force and separation energy). The high correlation confirms the relationship between the degree of NSC (represented by the adhesion) and the measured FRET signal (FRETeff).

FRETeff linearly increases with separation energy/adhesion (Figure 7), demonstrating that by functionalization of surfaces with FRET dye-nanolayers the degree of NSC between these surfaces can indeed be measured using FRET spectroscopy.

CONCLUSIONS

In this work, we demonstrate for the first time an innovative FRET system based on dye-nanolayer films prepared by physical vapor deposition, which was specifically developed for the measurement of NSC and its influence on adhesion. The dye-nanolayer films exhibit low roughness, uniform dye distribution, clear fluorescence intensities, and a spectral overlap, all factors which make them suitable for FRET.

For the FRET experiments and tensile testing, the dye-nanolayer films were bonded with increasing pressure to create different degrees of NSC and adhesion, corresponding to the applied load. The results showed that NSC measured by FRET and adhesion (separation energy per unit area) linearly increases with the employed pressure used to bond the dye-nanolayer films.

This validates the capacity of this unique FRET system for measurement of the degree of NSC between solid materials and the reliable correlation that can be established between FRET and adhesion.

The key innovation of this experimental method is that it can, in principle, be applied to arbitrary surfaces of soft and hard materials. Functionalizing surfaces with FRET dye-nanolayers is an actively novel approach to studying NSC using FRET spectroscopy. It can be applied on any sufficiently transparent substrate that can be used for the deposition of the Donor and Acceptor molecules. Also, other FRET pairs suitable for physical or chemical vapor deposition can be utilized. A further key feature of the method is that it uses a large area of observation, which is unique for determining NSC, and avoids problems with elaborate sample preparation and unstable statistics and reproducibility that are frequent for nanoscale imaging techniques.

Our investigations provide a unique experimental approach for the measurement of NSC, particularly useful to study adhesion between solid materials that can be of interest in all fields of engineering, contact mechanics, and tribology.

MATERIALS AND METHODS

pHema Thin Films Preparation. pHema (Sigma-Aldrich, Mw 20 000 Da, CAS:25249-16-5, USA) was dissolved to prepare a 10% (m/v) ethanol/water-Milli-Q mixture 95:5 (v/v) solution. Then, 500 μL of pHema solution were doctor bladed over polyvinyl chloride substrates to form 1.5 μm thin films using a bar film applicator (3 M BYK-Gardner GmbH, Geretsried, Germany) and left at room temperature for the evaporation of the solvents and consolidation of the films.

Donor and Acceptor Thin Films Preparation. The FRET pair (Figure 3A and 3B) of fluorescence molecules C120 (Sigma-Aldrich, CAS:26093-31-2, USA), and CDCF (Sigma-Aldrich, CAS:111843-78-8, Switzerland) were dissolved in ethanol to prepare 0.1 mM Donor and Acceptor (ratio of 1:1) solutions. Then, 100 μL of dye(s) solution were added to 500 μL of pHema solution.[10] The polymer−dye solutions were doctor bladed over polyvinyl chloride carrier substrates with a bar film applicator (3 M BYK-Gardner GmbH, Geretsried, Germany) [17] to form 1.5 μm Donor and Acceptor thin films (Figure 2A). To protect the dyes from unwanted quenching mechanisms or any other kind of light degradation, the dye solutions and thin films were prepared and handled in the dark and later protected in aluminum foil during the entire process and experiments.

Dye-Nanolayer Film Preparation − Physical Vapor Deposition. Donor and Acceptor molecules were deposited individually on pHema thin films in a custom-built PVD chamber. To deposit the dye nanolayer films, a vacuum chamber reactor equipped with a filament with a temperature controller was utilized (Figure 3D). The procedure was realized in four stages: (1) a pHema thin film was placed in the bottom of the reactor and a stainless-steel crucible, containing the dye (Donor or Acceptor) powder, and was positioned over the heating filament (Figure 3D). (2) The PVD chamber was degassed overnight to reach high vacuum. (3) The next day, the chamber was closed in a batch configuration, meaning that after heating the crucible, the reactor was separated from the vacuum pump, and the filament was heated to vaporize the dye (Donor or Acceptor). (4) After the deposition time (Table 2) the heating was turned off, the chamber was opened, and the dye-nanolayer film was

Table 2. PVD Conditions Used during the Preparation of the Dye Nanolayer Films

Dye Molecule	Pressure (mtorr)	Time (h)	Temperature (°C)	
			Substrate	Filament
C110-Donor	100	0.25	60	100
CDCF-Acceptor	100	6	60	120

collected (Figure 3D). To protect the dyes from unwanted quenching mechanisms or any other kind of light degradation, the dyes powder and films were prepared and handled in the dark and protected in aluminum foil.

Atomic Force Microscopy. The surface topography of the phema and dye-nanolayer films was investigated with an AFM (Tosca 400, Anton Paar, Austria). The measurements were performed to scan $500 \times 500\ nm^2$ topography images at ambient conditions (24 °C and 45% relative humidity). All measurements were obtained with an Olympus AC 240 TS probe with a nominal tip radius of 7 nm and a cantilever spring constant of about 2 N/m. The open-source software Gwyddion was used to process the images (for all samples, a second order polynomial background subtraction was performed) and determine the root-mean-square (RMS) roughness on at least three independent positions on each film.

Bonded Thin Films Preparation. For FRET spectroscopy, the bonding of the interface between the dye-nanolayer films was performed on 4 cm² of pure Donor (D), pure Acceptor (A), and/or pHema thin films without any dye (H), as demonstrated in Figure 7. The films were pressed at 1.5, 50, 100, 110, 120, 130, and 140 bar (hydraulic pressure PU30, V. Jessernigg & Urban, Graz, Austria) for 10 min.

FRET Spectroscopy. Spectra measurements of bonded dye-nanolayer films (Figure 6A-C) were recorded using a Fluorophotometer RF-5301PC (Shimadzu, Kyoto, Japan), at an excitation wavelength of 350 nm in a 45°/45° configuration, as demonstrated in Figure 6C.

FRET signals were detected from the bonded dye-nanolayer films and analyzed using Förster Theory.[14] The dye system presents a FRET working range distance that corresponds to $2R_0$ where R_0 is the Förster radius (nm). Following the instructions presented in the book FRET − Förster Resonance Energy Transfer: From Theory to Applications by Medintz and Hildebrandt (chapter 5, pages 106−122),[15] for random distributed fluorescence molecules point dipoles,[32] R_0 can be calculated via eq 1:

$$R_0 = \left(\frac{9 \ln(10)\ k^2 QY_{Donor} J}{128 \pi^5 N_A n^4} \right)^{1/6} \ (nm)$$

(1)

where N_A is Avogadro's constant ($6.02 \times 10^{20}\ mmol^{-1}$), k^2 is the orientation factor (2/3, considering randomly orientated dipoles during the FRET time[15,32]), n is the refractive index (1.5 for the thin films), QY_{Donor} is the Donor quantum yield (measured by the absolute method, $QY_{Donor} = 0.91$), and J is the overlap integral calculated with eq 2:

$$J = \int f_D(\lambda) \epsilon_A(\lambda) \lambda^4 d\lambda \ (nm^4 \cdot M^{-1} \cdot cm^{-1})$$

(2)

where f_D is the area normalized fluorescence intensity of the Donor, ε_A is the attenuation coefficient of the Acceptor ($M^{-1} \cdot cm^{-1}$), and λ is the wavelength (nm).

FRET efficiency (%) was calculated by the Acceptor Sensitization method[1] (eq 3). It is the ratio of the Acceptor spectral intensity peak value in the presence (I_{AD}) and in the absence (I_A) of the Donor (Figure 1).

To achieve appropriate FRET efficiency results, the direct luminescence of I_{AD} is subtracted from I_{AD}/I_A, and multiplied by the correct luminescence ratio of the Acceptor and Donor molar attenuation coefficients (ε_A and ε_D) at the excitation wavelength used for the FRET experiments.

$$FRETeff_{(Acceptor\ Sensitization)} = \left(\frac{I_{AD} - I_A}{I_A} \right) \left(\frac{\varepsilon_A}{\varepsilon_D} \right) (\%)$$

(3)

The Donor and Acceptor molar attenuation coefficients (ε, $M^{-1} \cdot cm^{-1}$) spectra are determined from the absorbance by Beer−Lambert's Law (eq 4):

$$A = \varepsilon c l$$

(4)

where A is the absorbance defined as the negative decadic logarithm of the measured transmittance, c is the concentration of the dye in the polymeric matrix (M), and l is the length of the light path, in this case, the thickness of the thin films (cm). Pure Donor and pure Acceptor thin film absorbance was measured with a Varian Cary, UV−vis spectrophotometer (Agilent Technologies, California, USA). To minimize the inner filter effect and deviations from Beer−Lambert's law, the optical density of the transmission measurements never exceeded 0.5 OD.

To calculate R_0 the instructions presented in the book FRET − Förster Resonance Energy Transfer: From Theory to Applications by Mendintz and Hildebrandt (section 5.5.2. pages 119−122) were followed.

Thin Film Separation Energy. Z-Direction tensile tests were performed in a ZwickRoell Z010 multipurpose tester (Georgia, USA) equipped with two steel bars, in which only the upper steel bar moves, driven by a linear motor. A double-sided adhesive tape is put on the upper and lower steel bars. After the sample is placed on the lower steel bar, the linear motor moves the upper steel bar down until it touches the sample. To guarantee good attachment of the sample at the steel bars, a defined compression force of 1.5 bar is applied. Then, the sample is pulled apart in the z-direction until it fails between the two polymer thin films. The force F with respect to separation distance x is recorded. The two main values for interpreting the tensile tests are the maximum tensile force and separation energy. The separation energy (J/cm²) is the integral of the force−distance curves, divided by the bonded area of the thin films.

■ ASSOCIATED CONTENT

ⓢ Supporting Information

The Supporting Information is available free of charge at https://pubs.acs.org/doi/10.1021/acsanm.4c01809.

Figure S1 − To employ FRET to measure NSC between surfaces, each interface needs to be labeled with the Donor or Acceptor dye (Figure S1). Due to the natural roughness of any surface, the NSC is not complete.[17] Instead, areas that look to be in full contact at the microscale end up revealing opens gaps at the nanometric scale.Thus, the areas in NSC are regularly overestimated when contact is evaluated at lower magnifications. However, a FRET signal only occurs within areas in NSC ($0.5R_0 - 2R$), for the open gaps above $2R$ no FRET can be found. Figure S2 − To validate the measurement of NSC using FRET, we measured the adhesion between the nanolayer films, which was created by the NSC between the surfaces, and correlate it to the measured FRET signals. Thus, the bonded films were separated by z-directional tensile testing to determine the separation energy and maximum adhesion force. The results showed that both parameters increase, with the increasing pressure applied to bonded dye-nanolayer films due to a higher degree of NSC and adhesion force. The separation energy per unit area was calculated by the integral of the tensile test force−displacement curves. (PDF)

■ AUTHOR INFORMATION

Corresponding Author

Mónica Gaspar Simões − AlmaScience Association, Pulp Research and Development for Smart and Sustainable Applications Madan Parque, Rua dos Inventores, 2825-182 Caparica, Portugal; orcid.org/0000-0003-2419-1545; Email: monica.simoes@almascience.pt

Authors

Katrin Unger − Silicon Austria Laboratories GmbH, 8010 Graz, Austria

Caterina Czibula − Institute of Bioproducts and Paper Technology, 8010 Graz, Austria

Anna Maria Coclite − Department of Physics, University of Bari Aldo Moro, 70125 Bari, Italy; orcid.org/0000-0001-5562-9744

Robert Schennach − Institute of Solid-State Physics, Graz University of Technology, 8010 Graz, Austria

Ulrich Hirn − Institute of Bioproducts and Paper Technology, 8010 Graz, Austria; orcid.org/0000-0002-1376-9076

Complete contact information is available at:
https://pubs.acs.org/10.1021/acsanm.4c01809

■ REFERENCES

(1) Persson, B. N. J. On the Mechanism of Adhesion in Biological Systems. *J. Chem. Phys.* **2003**, *118* (16), 7614−7621.

(2) Busuttil, K.; Geoghegan, M.; Hunter, C. A.; Leggett, G. J. Contact Mechanics of Nanometer-Scale Molecular Contacts: Correlation between Adhesion, Friction, and Hydrogen Bond Thermodynamics. *J. Am. Chem. Soc.* **2011**, *133* (22), 8625−8632.

(3) Le Saux, G.; Wu, M. C.; Toledo, E.; Chen, Y. Q.; Fan, Y. J.; Kuo, J. C.; Schvartzman, M. Cell-Cell Adhesion-Driven Contact Guidance and Its Effect on Human Mesenchymal Stem Cell Differentiation. *ACS Appl. Mater. Interfaces* **2020**, *12* (20), 22399−22409.

(4) Atkins, P.; de Paula, J. *Physical Chemistry for the Life Sciences*, 1st ed.; Oxford University Press: Oxford, 2006.

(5) Hirn, U.; Schennach, R. Comprehensive Analysis of Individual Pulp Fiber Bonds Quantifies the Mechanisms of Fiber Bonding in Paper. *Sci. Rep.* **2015**, *5* (July), No. 10503.

(6) Gong, G.; Zhou, C.; Wu, J.; Jin, X.; Jiang, L. Nanofibrous Adhesion: The Twin of Gecko Adhesion. *ACS Nano* **2015**, *9* (4), 3721−3727.

(7) Yang, C.; Persson, B. N. J. Molecular Dynamics Study of Contact Mechanics: Contact Area and Interfacial Separation from Small to Full Contact. *Phys. Rev. Lett.* **2008**, *100* (2), 1−4.

(8) Murphy, M. P.; Kim, S.; Sitti, M. Enhanced Adhesion by Gecko-Inspired Hierarchical Fibrillar Adhesives. *ACS Appl. Mater. Interfaces* **2009**, *1* (4), 849−855.

(9) Ciavarella, M.; Joe, J.; Papangelo, A.; Barber, J. R. The Role of Adhesion in Contact Mechanics. *J. R. Soc. Interface* **2019**, *16* (151), No. 20180738.

(10) Simões, M. G.; Urstöger, G.; Schennach, R.; Hirn, U. Quantification and Imaging of Nanoscale Contact with Förster Resonance Energy Transfer. *ACS Appl. Mater. Interfaces* **2021**, *13*, 19521.

(11) Simões, M. G.; Schennach, R.; Hirn, U. A System of FRET Dyes Designed to Assess the Degree of Nano-Scale Contact between Surfaces for Interfacial Adhesion. *J. Colloid Interface Sci.* **2024**, *653* (May 2023), 1642−1649.

(12) Simões, M. G.; Schennach, R.; H, U. A Pair of FRET Dyes Designed to Measure Nano-Scale Contact and the Associated Adhesion Force. *Mater. Sci.* **2023**, 1−17.

(13) Sahoo, H. Förster Resonance Energy Transfer - A Spectroscopic Nanoruler: Principle and Applications. *J. Photochem. Photobiol. C Photochem. Rev.* **2011**, *12* (1), 20−30.

(14) van der Meer, B. W. Förster Theory. In *FRET − Förster Resonance Energy Transfer*; John Wiley & Sons, Ltd, 2013; pp 23−62. DOI: 10.1002/9783527656028.ch03.

(15) Hildebrandt, N. How to Apply FRET: From Experimental Design to Data Analysis. In *FRET − Förster Resonance Energy Transfer*; John Wiley & Sons, Ltd: 2013; pp 105−163. DOI: 10.1002/9783527656028.ch05.

(16) Dexter, D. L. A Theory of Sensitized Luminescence in Solids. *J. Chem. Phys.* **1953**, *21* (5), 836−850.

(17) Persson, B. N. J.; Gorb, S. The Effect of Surface Roughness on the Adhesion of Elastic Plates with Application to Biological Systems. *J. Chem. Phys.* **2003**, *119* (21), 11437−11444.

(18) Benz, M.; Rosenberg, K. J.; Kramer, E. J.; Israelachvili, J. N. The Deformation and Adhesion of Randomly Rough and Patterned Surfaces. *J. Phys. Chem. B* **2006**, *110* (24), 11884−11893.

(19) Snell, N. E.; Rao, V. P.; Seckinger, K. M.; Liang, J.; Leser, J.; Mancini, A. E.; Rizzo, M. A. Homotransfer FRET Reporters for Live Cell Imaging. *Biosensors* **2018**, *8* (4), 89.

(20) Christopoulos, T. K.; Diamandis, E. P. Chapter 14 - Fluorescence Immunoassays. In *Immunoassay*; Diamandis, E. P., Christopoulos, T. K., Eds.; Academic Press: San Diego, 1996; pp 309−335. DOI: 10.1016/B978-012214730-2/50015-7.

(21) Shang, S. M.; Zeng, W. 4 - Conductive Nanofibres and Nanocoatings for Smart Textiles. In *Multidisciplinary Know-How for Smart-Textiles Developers*; Kirstein, T., Ed.; Woodhead Publishing Series in Textiles; Woodhead Publishing, 2013; pp 92−128. DOI: 10.1533/9780857093530.1.92.

(22) Aliofkhazraei, M.; Ali, N. 7.04 - PVD Technology in Fabrication of Micro- and Nanostructured Coatings. In *Comprehensive Materials Processing*; Hashmi, S., Batalha, G. F., Van Tyne, C. J., Yilbas, B., Eds.; Elsevier: Oxford, 2014; pp 49−84. DOI: 10.1016/B978-0-08-096532-1.00705-6.

(23) Danilov, D.; Hahn, H.; Gleiter, H.; Wenzel, W. Mechanisms of Nanoglass Ultrastability. *ACS Nano* **2016**, *10* (3), 3241−3247.

(24) Li, H.; Snow, P.; He, M.; Wang, P. I.; Wang, G. C.; Lu, T. M. Biaxially Textured Al Film Growth on CaF2 Nanostructures toward a Method of Preparing Single-Crystalline Si Film on Glass Substrates. *ACS Nano* **2010**, *4* (10), 5627−5632.

(25) Gong, C.; Huang, C.; Miller, J.; Cheng, L.; Hao, Y.; Cobden, D.; Kim, J.; Ruoff, R. S.; Wallace, R. M.; Cho, K.; Xu, X.; Chabal, Y. J. Metal Contacts on Physical Vapor Deposited Monolayer MoS2. *ACS Nano* **2013**, *7* (12), 11350−11357.

(26) Azizi, S.; Gholivand, M. B.; Amiri, M.; Manouchehri, I. DNA Biosensor Based on Surface Modification of ITO by Physical Vapor Deposition of Gold and Carbon Quantum Dots Modified with Neutral Red as an Electrochemical Redox Probe. *Microchem. J.* **2020**, *159* (September), No. 105523.

(27) Urstöger, G.; Steinegger, A.; Schennach, R.; Hirn, U. Spectroscopic Investigation of DCCH and FTSC as a Potential Pair for Förster Resonance Energy Transfer in Different Solvents. *PLoS One* **2020**, *15* (2), e0228543.

(28) Jin, T.; Uhlikova, N.; Xu, Z.; Zhu, Y.; Huang, Y.; Egap, E.; Lian, T. Competition of Dexter, Förster, and Charge Transfer Pathways for Quantum Dot Sensitized Triplet Generation. *J. Chem. Phys.* **2020**, *152* (21), No. 214702.

(29) Popp, L.; Scholz, R.; Kleine, P.; Lygaitis, R.; Lenk, S.; Reineke, S. High Performance Two-Color Hybrid TADF-Phosphorescent WOLEDs with Bimodal Förster and Dexter-Type Exciton Distribution. *Org. Electron.* **2019**, *75*, No. 105365.

(30) Medintz, I.; Hildebrandt, N. *FRET - Förster Resonace Energy Transfer: From Theory to Applications*, 1st ed.; Medintz, I.,

Hildebrandt, N., Eds.; WILEY-VCH Verlag: Weinheim, Germany, 2014.

(31) Urstöger, G.; Simoes, M. G.; Steinegger, A.; Schennach, R.; Hirn, U. Evaluating the Degree of Molecular Contact between Cellulose Fiber Surfaces Using FRET Microscopy. *Cellulose* **2019**, *26*, 7037−7050.

(32) Shaw, P. E.; Ruseckas, A.; Samuel, I. D. W. Distance Dependence of Excitation Energy Transfer between Spacer-Separated Conjugated Polymer Films. *Phys. Rev. B - Condens. Matter Mater. Phys.* **2008**, *78* (24), 1−5.